



Active noise control in a forced-air cooling system

R.A. de Callafon, J. Zeng, C.E. Kinney *

University of California, San Diego, Department of Mechanical and Aerospace Engineering, 9500 Gilman Drive, La Jolla, CA 92093-0411, USA

ARTICLE INFO

Article history:

Received 5 September 2008

Accepted 13 May 2010

Keywords:

Active noise control
Feedforward control
Parameter estimation
Digital filters
Control applications

ABSTRACT

This paper discusses the design methodology for the active noise control of sound disturbances in a forced-air cooling system. The active sound cancellation algorithm uses the framework of output-error based optimization of a linearly parametrized filter for feedforward sound compensation to select microphone location and demonstrate the effectiveness of active noise cancellation in a small portable data projector. Successful implementation of the feedforward based active noise controller on a NEC LT170 data projector shows a 20–40 dB reduction per frequency point in the spectrum of external noise of the forced-air cooling system can be obtained over a broad frequency range from 1 to 5 kHz. A total noise reduction (unweighted) of 9.3 dB is achieved.

© 2010 Elsevier Ltd. All rights reserved.

1. Introduction

Small electronic systems often require forced air-cooling to control the temperature of large power sensitive components in the system. Moving air through a fan provides an effective resource for cooling, but suffers from the drawbacks of noise due to turbulence and vibrations. In applications where external sound disturbances interfere with the environment, passive or active attenuation can be used to control sound emission of forced-air cooling systems (Gee & Sommerfeldt, 2003). Passive noise control is effective at reducing high frequency sound components but requires large amounts of absorption material to reduce low frequent noise signals (Bernhard, 2000; Gentry, Guigou, & Fuller, 1997; Hu & Lin, 2000). Especially for small electronic systems, this is not a viable solution.

Active noise control (ANC) can be used for sound reduction and can be particularly effective at lower frequency sound components. ANC allows for much smaller design constraints and has received attention in recent years (O'Brien, Pratt, & Downing, 2002; Sano & Terai, 2003) and many applications of active noise techniques can be found in the literature (e.g., Berkman & Bender, 1997; Cabell & Fuller, 1999; Esmailzadeh, Alasty, & Ohadi, 2002; Fuller & Von Flotow, 1995). The basic principle and idea behind ANC is to cancel sound by a controlled emission of a secondary opposite (out-of-phase) sound signal (Denenberg, 1992; Wang, Tse, & Wen, 1997).

In active noise cancellation systems with a relatively small amount of feedback from the control speaker to the pick-up microphone, called acoustic coupling, feedforward compensation provides an effective resource to create a controlled emission for sound attenuation. Algorithms based on recursive (filtered) least mean squares (LMS) minimization (Haykin, 2002) can be quite effective for the estimation and adaptation of feedforward based sound cancellation (Cartes, Ray, & Collier, 2002). To facilitate an output-error based optimization of the feedforward compensation, a linearly parametrized finite impulse response (FIR) filter has been used for the recursive estimation and adaptation.

Many other viable ANC structures exist, such as hybrid ANC (Yuan, 2004) which combines feedforward and feedback control. In this application, hybrid ANC is not practical, as an error microphone externally located on the device will pick up a significant amount of noise, limiting the ANC to feedforward. In the current work, the error microphone is used to evaluate the reference or pick-up microphone location only. The final noise control system uses one reference microphone and one control speaker. This was done to keep the number of sensors low and the signal-to-noise ratio high, which is desirable for product development.

In this paper the framework of output-error based optimization of a linearly parametrized filter for feedforward sound compensation is used to demonstrate the effectiveness of active noise cancellation in a small portable data projector depicted in Fig. 1. The projector in Fig. 1 is equipped with a shielded internal directional pick-up microphone to measure the sound created by the forced-air cooling of the projector's light bulb. Non-invasive small directional speakers located at the inlet and outlet grill of the data projector are used to minimize acoustic coupling and complete the active noise control system.

* Corresponding author. Tel.: +1 858 822 1763; fax: +1 858 822 3107.

E-mail addresses: callafon@ucsd.edu (R.A. de Callafon), jzeng@ucsd.edu (J. Zeng), cekinney@gmail.com (C.E. Kinney).

URL: <http://www.mae.ucsd.edu/research/callafon/> (R.A. de Callafon).

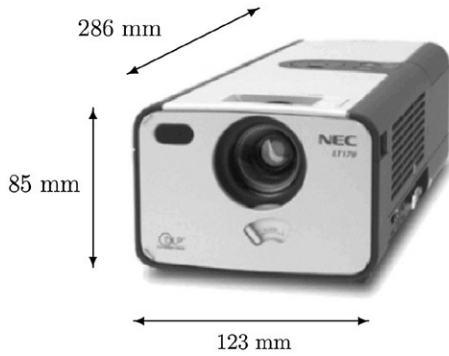


Fig. 1. Dimensions of NEC LT170 data projector with inlet side grill for forced-air cooling system.

The feedforward control algorithm for active noise control presented in this paper is based on the estimation of a generalized finite impulse response filter (Zeng & de Callafon, 2003). Generalized or orthogonal FIR models have been proposed in Heuberger, Van Den Hof, and Bosgra (1995) and exhibit the same linear parametrization as a standard FIR filter. Combined with an affine optimization of the filter coefficients, an optimal feedforward compensator for noise cancellation can be obtained for the data projector. Implementation of the feedforward based ANC on the data projector shows a 20–40 dB reduction of external noise of the forced-air cooling system over the frequency range from 1 to 5 kHz.

2. Active noise control

2.1. Analysis of feedforward compensation

In a scalar feedforward noise compensation, an (amplified) signal $u(t)$ from an internal pick-up microphone is fed into a feedforward compensator F that controls the signal $u_c(t)$ to a control speaker for sound compensation. In order to analyze the design of a feedforward compensator F for active noise cancellation, consider the signal $e(t)$ that reflects the combined effect of sound due to external disturbance and control speaker.

The objective of the ANC system is to minimize the signal $e(t)$ and an error microphone can be used to measure $e(t)$ and monitor the performance of the ANC system. The dynamical relationship between the discrete time sampled signals in the ANC system can be characterized by difference equations, where the operator q is used to denote a unit sample delay $qu(t) = u(t+1)$. The dynamic relationship between the control input $u_c(t)$, the sound disturbance $u(t)$, and the error signal $e(t)$ is shown in Fig. 2. From this figure, it is clear that the error signal can be characterized by

$$e(t) = H(q)u(t) + G(q)u_c(t) \quad (1)$$

where $H(q)$ is a stable filter in the 'primary path' and $G(q)$ is a stable filter in the 'secondary path' of the ANC system. $H(q)$ and $G(q)$ characterize the discrete time dynamic aspects of the sound propagation from the sound disturbance and control input, respectively, to the error signal $e(t)$.

The sound disturbance $u(t)$ of the forced-air cooling system measured at the pick-up microphone is characterized by

$$u(t) = W(q)n(t)$$

where $n(t)$ is a zero-mean white noise signal with variance $E\{n(t)^2\} = \lambda$ and $W(q)$ is a (unknown) stable and stably invertible noise filter. The combination of a zero-mean and filtered white noise signal $u(t)$ allows for a characterization of a rich class

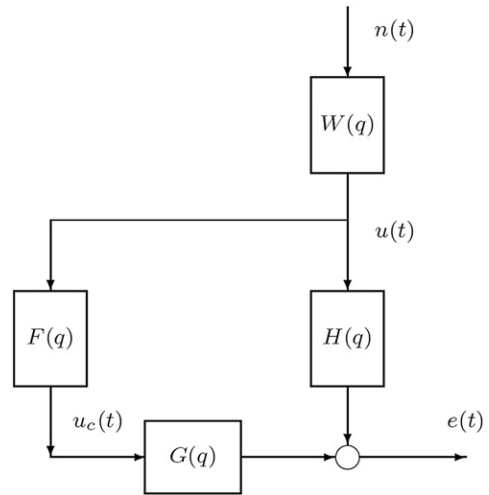


Fig. 2. Block diagram of the dynamic relationship between the control input $u_c(t)$, the sound disturbance $u(t)$, and the error signal $e(t)$.

of random sound disturbances for which the discrete time spectrum $\lambda|W(e^{j\omega})|^2$ can be modeled by a spectral decomposition (Ljung, 1999). In case the sound disturbance $u(t)$ itself is not influenced by the feedforward sound compensation $u_c(t) = F(q)u(t)$, the performance signal $e(t)$ can easily be described by

$$e(t) = W(q)[H(q) + G(q)F(q)]n(t) \quad (2)$$

and is a stable map, provided the feedforward compensator $F(q)$ is stable. Absence of a correlation between $u_c(t)$ and $u(t)$ given by $u(t) = G_c(q)u_c(t)$ requires a well-designed ANC system that minimizes the acoustic coupling¹ $G_c(q)$. For the ANC application of the data projector discussed in this paper, acoustic coupling is minimized by small directional speakers located at the outside of the data projector. As a result, the effect of acoustic coupling is not considered in the remaining part of the paper. However, if acoustic coupling is present then the method presented in de Callafon and Zeng (2006) can be used to eliminate the feedback.

In case the transfer functions in (2) are known, an ideal feedforward compensator $F(q) = F_i(q)$ can be obtained in case

$$F_i(q) = -\frac{H(q)}{G(q)} \quad (3)$$

is a stable and causal transfer function. The solution of $F_i(q)$ in (3) assumes full knowledge of $G(q)$ and $H(q)$. Moreover, the filter $F_i(q)$ may not be a causal or stable filter due to the dynamics of $G(q)$ and $H(q)$ that dictate the solution of the feedforward compensator $F_i(q)$. An approximation of the feedforward filter $F_i(q)$ can be made by an output-error based optimization that aims at finding the best causal and stable approximation $F(q)$ of the ideal feedforward compensator in $F_i(q)$ in (3).

The output-error based approximation can be characterized by examining the variance of the discrete time error signal $e(t)$ in (2) that is given by

$$\frac{\lambda}{2\pi} \int_{-\pi}^{\pi} |W(e^{j\omega})|^2 |H(e^{j\omega}) + G(e^{j\omega})F(e^{j\omega})|^2 d\omega$$

where λ denotes the variance of $n(t)$. In case variance minimization of the error microphone signal $e(t)$ is required for ANC, the

¹ Acoustic coupling is a feedback term from the control speaker to the pick-up microphone that can cause poor performance and instabilities if present and not accounted for in the design of the feedforward compensator.

optimal feedforward controller is found by the minimization

$$\min_{\theta} \int_{\omega=-\pi}^{\pi} |L(e^{j\omega}, \theta)|^2 d\omega := \min_{\theta} \|L(q, \theta)\|_2, L(q, \theta) = W(q)[H(q) + G(q)F(q, \theta)] \quad (4)$$

where the parametrized filter $F(q, \theta)$ is required to be a causal and stable filter.

The minimization in (4) is a standard 2-norm based feedback control and model matching problem (Bai & Lin, 1997; Hu, Yu, & Hsieh, 1998) that can be solved in case $W(q)$, $G(q)$ and $H(q)$ are known. Unfortunately, the discrete time dynamic relation between the signals $e(t)$, $u(t)$ and $u_c(t)$ is unknown. Moreover, even with a fixed location of the control speaker, the transfer functions $W(q)$, $G(q)$ and $H(q)$ depend on the location of the microphones of the ANC system.

2.2. Optimal location of pick-up microphone

To minimize the acoustic coupling from the control speaker to the pick-up microphone in the ANC system of the data projector, a directional control speaker is placed at the external opening of the projector and directed outwards. As a verification step, the correlation between the pick-up microphone and control speaker was calculated and seen to be small at each potential location of the pick-up microphone. If there is an undesired amount of acoustic coupling then the method described in de Callafon and Zeng (2006) can be used to eliminate the feedback. Due to space limitations in the small portable projector, only limited space is available for the control speaker. Furthermore, the error microphone is used only to temporarily measure the error signal $e(t)$, but will not be part of the ANC as only feedforward compensation will be used for sound compensation.

If design freedom is available for the location of the pick-up microphone, then it should be exploited to develop a well-performing ANC system. In order to study the performance of the ANC system, consider a certain location of the pick-up microphone in the ANC system. For that specific location, the transfer functions $H(q)$, $G(q)$ in (1) are fixed, but unknown. As a result, the performance of the ANC system solely depends on the design freedom in the feedforward compensator $F(q, \theta)$ to minimize the error signal $e(t)$.

The design freedom of feedforward compensator $F(q, \theta)$ is restricted by the parametrization of $F(q, \theta)$ in terms of the filter coefficients θ . A direct optimization of the feedforward compensator $F(q, \theta)$ can be performed by considering the parametrized error signal $e(t, \theta)$

$$e(t, \theta) = H(q)u(t) + F(q, \theta)G(q)u(t) \quad (5)$$

Definition of the signals

$$y(t) := H(q)u(t), \quad u_f(t) := -G(q)u(t) \quad (6)$$

reduces (5) to

$$e(t, \theta) = y(t) - F(q, \theta)u_f(t) \quad (7)$$

for which the minimization

$$\min_{\theta} \frac{1}{N} \sum_{t=1}^N e^2(t, \theta) \quad (8)$$

to compute the optimal feedforward filter $F(q, \theta)$ is a standard output-error (OE) minimization problem in a prediction error framework (Ljung, 1999).

Using the fact that the variance of the pick-up microphone signal $u(t)$ satisfies $\|u\|_2 = |W(q)|^2 \lambda$, the minimization of (8)

for $\lim_{N \rightarrow \infty}$ can be rewritten into the frequency domain expression

$$\min_{\theta} \int_{\pi}^{-\pi} |W(e^{j\omega})|^2 |H(e^{j\omega}) + G(e^{j\omega})F(e^{j\omega}, \theta)|^2 d\omega \quad (9)$$

using Parseval's theorem (Ljung, 1999). It can be observed that (9) and (4) are equivalent and the standard output-error (OE) minimization problem in (8) can be used to compute the optimal feedforward filter $F(q, \theta)$, provided $y(t)$ and $u_f(t)$ in (6) are available.

For a specific location of the pick-up microphone, the signals in (6) are easily obtained by performing a series of two experiments. The two experiments simply measure the pick-up and error microphone signals $u(t)$ and $e(t)$:

- (1) The first experiment is done without feedforward compensation. Hence, $F(q, \theta) = 0$ and the error microphone signal $e_1(t)$ satisfies
$$e_1(t) = H(q)u(t) \quad (10)$$

In addition, the pick-up microphone

$$\tilde{u}(t) := u(t) + v(t) \quad (11)$$

is measured, where $v(t)$ indicates possible measurement noise on the pick-up microphone signal. Such noise might arise in case the pick-up microphone is placed in the air flow of the forced-air cooling system. This results in additional disturbances on the pick-up microphone signal that need to be considered in the optimal location of the microphone.

- (2) The second experiment is done with the forced air-cooling system turned off, eliminating the presence of the external sound disturbance. Subsequently, the measured input microphone signal $-\tilde{u}(t)$ in (11) from the first experiment is applied to the control speaker, yielding the error microphone signal

$$e_2(t) = -G(q)\tilde{u}(t) = -G(q)u(t) - G(q)v(t) \quad (12)$$

With $u_f(t) := -G(q)u(t)$, (7) can be written as

$$e(t, \theta) = e_1(t) - F(q, \theta)e_2(t) - F(q, \theta)G(q)v(t) \quad (13)$$

Alternatively, both experiments can be combined by using a filtered input signal $u_f(t)$ that is based on an estimated model $\hat{G}(q)$ of $G(q)$. Because $G(q)$ is fixed once the location of the control speaker is determined, an initial off-line estimation can be used to estimate a model for $G(q)$ to construct the filtered input signal $u_f(t)$. The use of an estimated transfer function for filtering purposes in recursive and adaptive estimation is common practice in most filtered least mean squares algorithms (Cartes et al., 2002). Similar approaches are also found in identification algorithms that provide unbiased estimates of models on the basis of closed-loop experimental data.

In the absence of the noise $v(t)$ on the input microphone, the minimization of $e(t, \theta)$ in (13) is equivalent to the minimization of $e(t, \theta)$ in (7). As a result, the obtainable performance of the ANC for a specific location of the pick-up microphone can be evaluated directly on the basis of the error microphone signals $e_1(t)$ and $e_2(t)$ from the first and second experiment, respectively. The result is summarized in the following proposition.

Proposition 1. *The performance of the feedforward ANC system for a specific location of the pick-up microphone is characterized by $V_N(\hat{\theta})$. The numerical value of $V_N(\hat{\theta})$ is found by measuring $e_1(t)$ and $e_2(t)$ for $t = 1, \dots, N$ as described by the experiments above, and solving an OE model estimation problem*

$$\hat{\theta} = \min_{\theta \in \mathbb{R}^d} V_N(\theta)$$

with

$$V_N(\theta) := \frac{1}{N} \sum_{t=1}^N \varepsilon^2(t, \theta)$$

and

$$\varepsilon(t, \theta) := e_1(t) - F(q, \theta) e_2(t) \quad (14)$$

for a finite size d parameter $\theta \in \mathbb{R}^d$ that represents the coefficients of a finite order filter $F(q, \theta)$.

A finite number d of filter coefficients is chosen in Proposition 1 to provide a feasible optimization of the filter coefficients. It should be noted that an FIR parametrization

$$F(q, \theta) = \sum_{k=0}^{p-1} \theta_k q^{-k} \quad (15)$$

leads to an affine optimization of the filter coefficients. Although FIR filter representations require many filter coefficients θ_k for an accurate design of a feedforward filter, the FIR filter can be used at first only to evaluate the possible performance of the ANC for a specific pick-up microphone location. To anticipate on the remaining results of the paper it can be said here that such an affine optimization will be exploited by parameterizing the feedforward filter using a generalized FIR filter that uses an general orthogonal expansion of basis functions to construct the feedforward filter for the actual implementation of the ANC system.

As a final note it can be observed that the pick-up microphone is possibly subjected by a noise $v(t)$. It can be seen that the minimization of $\varepsilon(t, \theta)$ in (14) is equivalent to (8) with a noise $G(q) v(t)$ disturbing the output $e_2(t)$. However, the noise is correlated with the input $e_1(t)$ and correlated noise on the input leads to bias in OE minimization (Ljung, 1999). This directly gives rise to a performance deterioration of the feedforward ANC system in case the pick-up microphone is placed unshielded inside the air flow of the forced-air cooling system.

3. Feedforward implementation with generalized FIR

3.1. Generalized FIR filter

In general, the OE minimization of (14) is a non-linear optimization but reduces to a convex optimization problem in case $F(q, \theta)$ is parametrized linearly in the parameter θ . Linearity in the parameter θ is also favorable for on-line recursive estimation of the filter, as convergence to optimal and unbiased feedforward compensators is obtained irrespective of the coloring of the noise on the data (Ljung, 1999). A linear parametrization of $F(q, \theta)$ can be obtained by using a FIR filter (15), but many parameters θ_k are required to approximate an optimal feedforward controller for a complex ANC with many lightly damped resonances. To improve these aspects, generalized FIR filters can be used.

To improve the approximation properties of the feedforward compensator in ANC, the linear combination of tapped delay functions q^{-1} in the FIR filter of (15) are generalized to

$$F(q, \theta) = D + \sum_{k=0}^N L_k V_k(q), \quad \theta = [D \ L_0 \ \dots \ L_N]$$

where D is a possible direct feed-through term and $V_k(q)$ are linearly weighted L_k generalized (orthonormal) basis functions (Heuberger et al., 1995) that contain knowledge of the dynamics of the optimal feedforward controller for the ANC system. The basis functions are a generalization of $V_k(q) = q^{-k}$ used in a FIR filter and guarantee the causality and stability of the feedforward

compensator for implementation purposes. For details on the construction of the functions $V_k(q)$ one is referred to Heuberger et al. (1995). A short overview of the properties is given here where the concepts of inner functions play an essential role.

Corollary 1. Let the pair (A, B) be the state matrix and input matrix of an input balanced state space realization with a McMillan degree $n > 0$, and with $\text{rank}(B) = m$. Then matrices (C, D) can be constructed according to

$$C = UB^*(I_n + A^*)^{-1}(I_n + A)$$

$$D = U[B^*(I_n + A^*)^{-1}B - I_m]$$

where $(\cdot)^*$ indicates complex conjugate transpose of a matrix and $U \in \mathbb{R}^{m \times m}$ is any unitary matrix. This yields a square $m \times m$ inner transfer function $P(q) = D + C(qI - A)^{-1}B$, where (A, B, C, D) is a minimal balanced realization.

As $P(q)$ is analytic outside and on the unit circle, it has a Laurent series expansion

$$P(q) = \sum_{k=0}^{\infty} P_k q^{-k}$$

which yields a set of orthonormal functions P_k (Heuberger et al., 1995). Orthonormality of the set P_k can be seen by z-transformation of P_k :

$$\frac{1}{2\pi} \int_{-\pi}^{\pi} P_i(e^{j\omega}) P_k^T(e^{-j\omega}) d\omega = \begin{cases} I, & i = k \\ 0, & i \neq k \end{cases}$$

With the notion of an input balanced state space model and the inner transfer function $P(q)$, the concept of an orthonormal basis expansion can be defined. Consider $V_0(q) := (qI - A)^{-1}B$ and

$$V_k(q) := (qI - A)^{-1} B P^k(q) = V_0(q) P^k(q) \quad (16)$$

then a generalized FIR filter can be constructed that consists of a linear combination of the basis functions $\sum_{k=0}^N L_k V_k(q)$. This yields a generalized FIR filter that can be augmented with standard delay functions

$$F(q, \theta) = q^{-n_k} \left[D + \sum_{k=0}^N L_k V_0(q) P^k(q) \right], \quad \theta = [D \ L_0 \ \dots \ L_N] \quad (17)$$

to incorporate a delay time of n_k time steps in the feedforward compensator. The parametrization of the feedforward compensator in (17) exhibits the same favorable properties of a linear parametrization found in a standard FIR filter. As a result the optimization in (14) will be an affine optimization to find the optimal feed forward compensator for the ANC system. The advantage lies in the additional information on the dynamics of the basis functions $V_k(q)$ that can be incorporated to further improve the accuracy of the feedforward filter in the approximation of $F_i(q)$ in (3).

3.2. Construction of basis functions and implementation

To facilitate the use of the generalized FIR filter for feedforward based ANC control, the basis function $V_k(q)$ of $F(q, \theta)$ in (16) have to be selected. The basis functions are based on the state space matrices (A, B) of an initial model of $F(q, \theta)$ from which the inner transfer functions $P(q)$ are created. A low order model for the basis functions will suffice, as the generalized FIR model will be expanded on the basis of $V_k(q)$ to improve the accuracy of the feedforward compensator.

An initial low order model for the feedforward compensator is obtained from the analysis of the performance of the ANC system mentioned in Proposition 1. The optimization (14) to evaluate the optimal location of the pick-up microphone can be used to

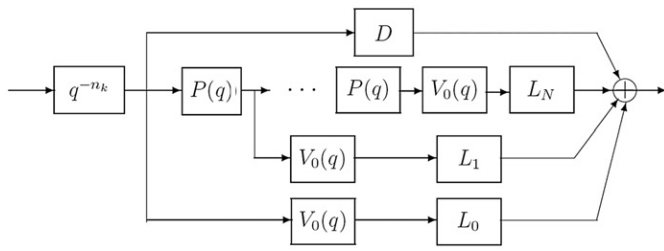


Fig. 3. Basic structure of generalized FIR filter.

estimate a low order model $F(q, \hat{\theta}), \hat{\theta} \in \mathbb{R}^d$. The initial low order IIR model $F(q, \hat{\theta})$ can be used to generate the basis functions $V_k(q)$ of the generalized FIR filter of the feedforward compensator $F(q, \theta)$ in (17). With the basis functions in place, the optimization (14) for the parameterization (17) becomes an affine optimization problem that can be used to further improve the accuracy of the feedforward based ANC system.

A block diagram of the generalized FIR filter $F(q)$ in (17) is depicted in Fig. 3 and it can be seen that it exhibits the same tapped delay line structure found in a conventional FIR filter, with the difference of more general basis functions $V_k(q)$.

An important property and advantage of the generalized FIR filter is that knowledge of the (desired) dynamical behavior can be incorporated in the basis function $V_k(q)$. Without any knowledge of desired dynamic behavior, the trivial choice of $V_k(q) = q^{-k}$ reduces the generalized FIR filter to the conventional FIR filter. If a more elaborate choice for the basis function $V_k(q)$ is incorporated, then (17) can exhibit better approximation properties for a much smaller number of parameters N than used in a conventional FIR filter. Consequently, the accuracy of the feedforward controller $F(q, \theta)$ in the approximation of the ideal forward filter in (4) will substantially increase.

4. Feedforward ANC on data projector

4.1. Location of pick-up microphone

To illustrate the effectiveness of feedforward based active noise control using a feedforward filter parametrized by a orthonormal basis function expansion, the NEC LT170 data projector depicted in Fig. 1 was used. The small and portable projector is equipped with a shielded internal directional pick-up microphone to measure the sound created by the forced-air cooling of the projector's light bulb. Non-invasive small directional speakers located at the inlet grill minimize acoustic coupling in the data projector and will be used to reduce ambient noise from the projector due to the forced air-cooling system.

The location of the inlet grill of the data projector determines the location of the control speakers. However, inside the projector there are several small areas close to the air cooling fan where a directional pick-up microphone could be placed. An overview of the design space to place a microphone inside the projector has been indicated in Fig. 4, where the top of the projector has been removed for visualization purposes.

The error microphone is placed 25 cm away from the inlet grill of the projector and experimental data of the NEC data projector is gathered in an anechoic room located at the System Identification and Control Laboratory at UCSD at a sampling frequency of 20kHz. As indicated in Fig. 4, four possible locations are considered for the location of the pick-up microphone.

For each location experiments were done according to Proposition 1 to observe the error and pick-up microphone signals. In order to predict the performance of the feedforward

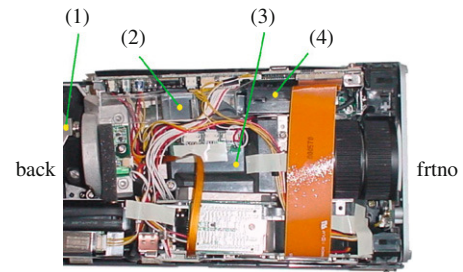


Fig. 4. Top view of NEC LT170 data projector for ANC design with possible locations for pick-up microphone: (1) in proximity of light bulb, (2) in air flow channel, (3) in central part of projector, and (4) in close proximity of cooling fan.

Table 1

Results of affine optimization (14) using a 40th order FIR model $F(q, \theta)$ for the pick-up microphone locations in Fig. 4.

Location	$var\{e_1(t)\}$	$V_N(\hat{\theta})$	Reduction (%)
(1)	1.8612×10^{-4}	1.4171×10^{-4}	76
(2)	1.8535×10^{-4}	1.7725×10^{-4}	96
(3)	1.8599×10^{-4}	1.0421×10^{-4}	56
(4)	1.8609×10^{-4}	1.7282×10^{-4}	93

based ANC system for each pick-up microphone location, a 40th order FIR model $F(q, \theta)$ was estimated by the affine optimization (14). A high order FIR filter was chosen to find good approximation results of the achievable optimal filter via the affine optimization. It should be noted that the 40th order FIR model is not the actual feedforward filter that would be implemented as the ANC feedforward compensator; only the value of the criterion function $V_N(\hat{\theta})$ was used to predict the performance of the ANC system for the different pick-up microphone locations. The results have been summarized in Table 1.

The variance of the error microphone signal

$$var\{e_1(t)\} := \frac{1}{N} \sum_{t=1}^N e_1^2(t)$$

during the first experiment $e(t) = e_1(t)$ is independent of the pick-up microphone location, but small variations occur due to experimental variabilities. For normalization purposes, the value of the criterion function

$$V_N(\hat{\theta}) = \frac{1}{N} \sum_{t=1}^N \varepsilon(t, \hat{\theta})^2, \quad \varepsilon(t, \hat{\theta}) = e_1 - F(q, \hat{\theta})e_2(t)$$

is compared with the variance $var\{e_1(t)\}$ to indicate the improvement the simulated noise $\varepsilon(t, \hat{\theta})$ of the error microphone signal due to the feedforward compensator $F(q, \hat{\theta})$. Thus, the reduction percentage is given by

$$\frac{V_N(\hat{\theta})}{var\{e_1(t)\}} \times 100$$

It can be observed from Table 1 that positioning of the pick-up microphone in the center location of the projector gives far superior feedforward ANC performance than the other locations. As expected, the bad performance at location (2) is due to a large noise contribution $v(t)$ on the pick-up microphone signal in (11) by placing the microphone in the air flow of the air-cooling system. Similarly, the close proximity of the microphone to the fan in location (4) causes the microphone to pick up residual vibrations, disturbances that deteriorate feedforward performance, and due to the proximity of the fan to the source, may pick up non-propagating noise.

4.2. Estimation and implementation of feedforward ANC

With the input microphone at the center location (3) in Fig. 4 of the data projector, experimental data of the error microphone signal $e_1(t)$ and $e_2(t)$ and input microphone $u(t)$ were gathered according to the two experiments outlined in (10) and (12). The microphone signals sampled at 20 kHz can now be used to estimate a low order IIR model $\tilde{F}(q) = F(q, \hat{\theta})$ via output error optimization to create the basis function $V_k(q)$ in (16) for the generalized FIR filter parametrization of the feedforward controller.

The estimation results of an estimated 6th order model $\tilde{F}(q)$ is shown in Fig. 5. For validation and illustration purposes, the Bode plot of the 6th order model $\tilde{F}(q)$ in Fig. 5 is compared with the frequency domain estimate $F(j\omega)$ defined by

$$F(j\omega) := -\frac{\hat{H}(j\omega)}{\hat{G}(j\omega)} \quad (18)$$

over the frequency grid $\omega \in \Omega$, where $\Omega = \{0, 3.125, 2 \cdot 3.125, \dots, 10e3\}$ Hz consists of 3201 points. In (18), the frequency response estimates $\hat{H}(j\omega)$ and $\hat{G}(j\omega)$ are found by spectral analysis (Priestley, 1981) using Welch's method and the amplitude Bode plots of $\hat{H}(j\omega)$ and $\hat{G}(j\omega)$ along with their coherence plots have been depicted individually in Fig. 6. Specifically, $\hat{H}(j\omega)$ is found via

$$\hat{H}(j\omega) = \hat{\Phi}_{eu}^N(j\omega) / \hat{\Phi}_{ee}^N(j\omega), \quad \omega \in \Omega$$

where $\hat{\Phi}_{eu}^N(j\omega)$ denotes the N -point one-sided discrete fourier transform (DFT) of an unweighted averaged cross-covariance function

$$\hat{\Phi}_{eu}^N(j\omega) = \sum_{\tau=0}^{N-1} \hat{R}_{eu}^N(\tau) e^{-j\omega\tau}, \quad \omega \in \Omega$$

where the averaged cross-covariance function $\hat{R}_{eu}^N(\tau)$ is found via

$$\hat{R}_{eu}^N(\tau) = \frac{1}{n} \sum_{k=1}^n \hat{R}_{eu,k}^N(\tau), \quad \hat{R}_{eu,k}^N(\tau) = \frac{1}{N} \sum_{t=0}^{N-1} e(t)u(t-\tau)$$

using n averages on non-overlapping data sequences of $e(t)$ and $u(t)$. A similar procedure was used for the frequency response estimate $\hat{G}(j\omega)$ using the output signal $e(t)$ of the error microphone and the input signal $u_c(t)$ to the control speaker.

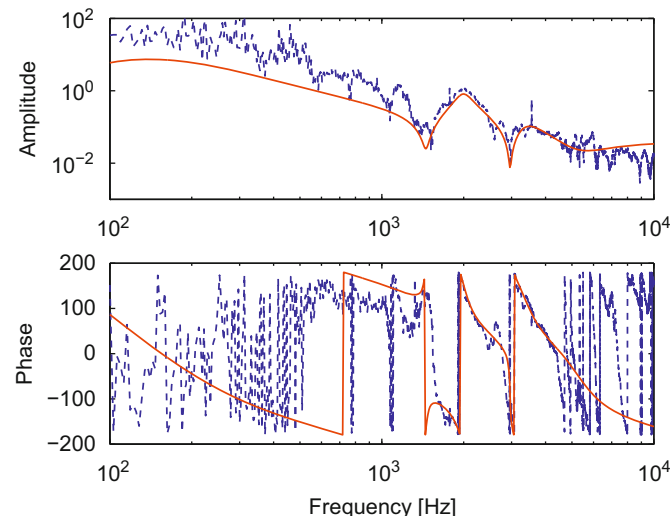


Fig. 5. Amplitude (top) and phase (bottom) Bode plot of frequency domain estimate $F(j\omega)$ (dashed) defined in (18) and 6th order parametric model $\tilde{F}(q)$ (solid).

The frequency response estimates were done over $n=20$ averages using $N=6400$ data points over the frequency grid Ω . From Fig. 5 it can be observed that the 6th order model $\tilde{F}(q)$ only models the main resonance modes of $H(q)/G(q)$ needed to capture the main dynamics of the poles of the optimal feedforward filter for active sound compensation.

The information of the initial 6th order feedforward filter $\tilde{F}(q)$ can be used to create the basis functions $V_k(q)$ of the generalized FIR filter in (17). With the basis functions in place, the optimization (14) for the parameterization (17) becomes an affine optimization problem that can be used to further improve the accuracy of the feedforward based ANC system, while avoiding high order FIR models for feedforward compensation. Estimation results lead to an 24th order generalized FIR model

$$\hat{F}(q) = F(q, \hat{\theta}) = \sum_{k=1}^4 \hat{L}_k V_k(q)$$

where $V_k(q)$ are the basis functions generated by the initial 6th order feedforward filter $\tilde{F}(q)$.

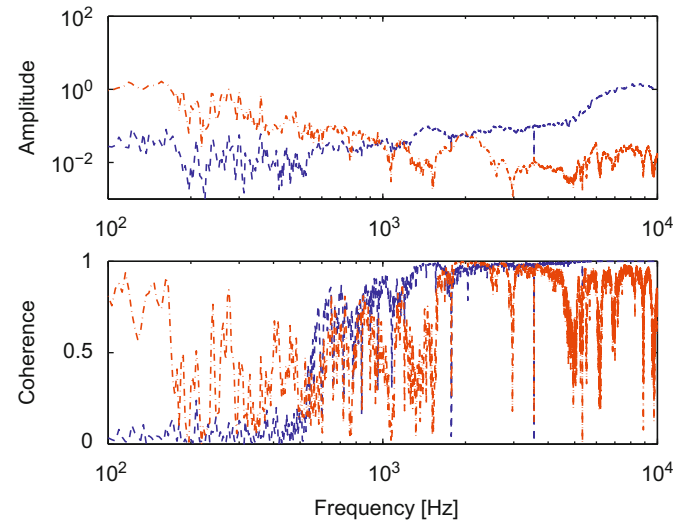


Fig. 6. Bode amplitude (top) and coherence (bottom) plot of frequency domain estimate $H(j\omega)$ (dashed) and $G(j\omega)$ (dashed-dotted).

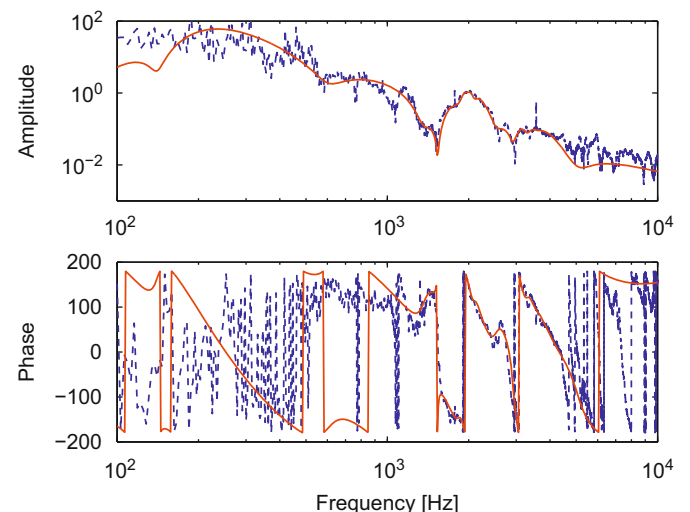


Fig. 7. Amplitude (top) and phase (bottom) Bode plot of frequency domain estimate $F(j\omega)$ (dashed) defined in (18) and 24th order generalized FIR filter $\hat{F}(q)$ (solid).

The 24th order generalized FIR filter $\hat{F}(q)$ shows promising results for the feedforward active sound compensation of the forced air-cooling system in the NEC LT170 data projector. To illustrate the performance of the filter, first consider the comparison of the Bode plot of the 24th order generalized FIR filter $\hat{F}(q)$ with the frequency domain estimate $\hat{F}(j\omega)$ in Fig. 7. Compared with the Bode plot of $\hat{F}(q)$ in Fig. 5, it can be seen that a better approximation is obtained.

The performance of the feedforward filter is also confirmed by the digital implementation of the filter. Using a Pentium based personal computer with equipped with a MultiQ3 12 bit signed AD/DA card, the 24th order filter can be implemented at a sampling frequency of 20 kHz sampling using the filter line structure depicted in Fig. 3. With the series connection of four 6th order basis functions $V_k(q)$, the 24th order generalized FIR filter is realized with a similar structure as a tapped delay line in a conventional FIR filter. Application of the feedforward filter for the active noise cancellation of sound in the data projector leads to the experimental data depicted in Fig. 8.

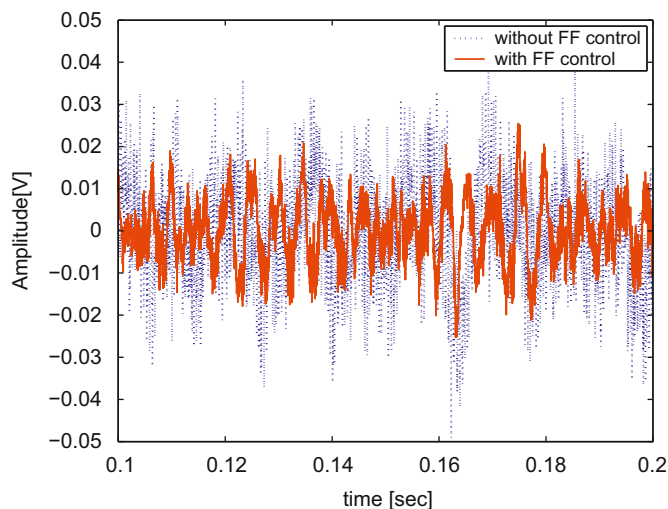


Fig. 8. Time trace of error microphone signal without (dotted) and with (solid) feedforward based active noise control. The feedforward control reduced the noise by 9.3 dB.

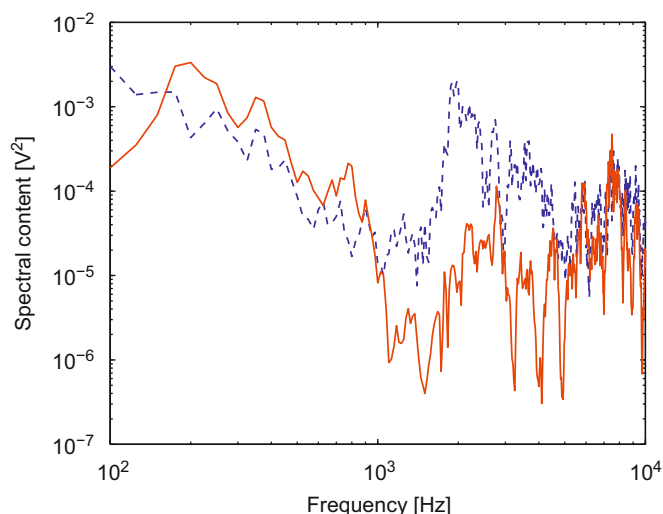


Fig. 9. Estimate of spectral contents of error microphone signal $e(t)$ without ANC (dashed) and with ANC using 24th order generalized FIR filter (solid), resulting in a 9.3 dB improvement.

The performance of the ANC system is confirmed by the estimates of the spectral contents of the microphone error signal $e(t)$ plotted in Fig. 9. The spectral content of the error microphone signal has been reduced significantly by the feedforward filter in the frequency range from 1 to 5 kHz, a frequency range that is particularly important in an A-weighting specification commonly used for the measurement of environmental and industrial noise. The experimental data depicted in Figs. 8 and 9 leads to a measured (unweighted) improvement of 9.3 dB.

5. Conclusions

Forced-air cooling systems move air through a fan to provide an effective resource for cooling of sensitive electronic components. The drawbacks of noise due to turbulence and vibrations in the air cooling system can be reduced by deploying an active noise control algorithm to reduce the external sound. This paper presents a methodology for the active noise control of sound disturbances in a forced-air cooling system found in data projector. Application of the design methodology on a NEC LT170 data projector shows the success of feedforward based noise cancellation in a small electronic system with high demands on the forced-air cooling system.

The methodology for ANC presented in this paper is based on feedforward compensation of sound by means of a pick-up microphone and a well-tuned feedforward filter. In the presence of small acoustic coupling, the methodology formulates an explicit criterion for the evaluation of the performance of the ANC system for different locations of the pick-up microphone. To facilitate data-based optimization of the feedforward filter, the filter is parameterized using a generalized FIR filter. The generalized FIR filter uses knowledge of the dynamics of the feedforward propagation of sound to construct a set of basis functions. For a much smaller number of filter coefficients than used in a conventional FIR filter, an elaborate choice for the basis function yields improved filter approximations for feedforward noise cancellation.

References

- Bai, M., & Lin, H. (1997). Comparison of active noise control structures in the presence of acoustical feedback by using the h_∞ synthesis technique. *Journal of Sound and Vibration*, 206(4), 453–471.
- Berkman, E., & Bender, E. (1997). Perspectives on active noise and vibration control. *Sound and Vibration*, 31, 80–94.
- Bernhard, R. (2000). Strategies for active and passive noise control. *Canadian Acoustics*, 28, 8–9.
- Cabell, R., & Fuller, C. (1999). A principal component algorithm for feedforward active noise and vibration control. *Journal of Sound and Vibration*, 227, 159–181.
- Cartes, D., Ray, L., & Collier, R. (2002). Experimental evaluation of leaky least-mean-square algorithms for active noise reduction in communication headsets. *Journal of the Acoustical Society of America*, 111, 1758–1771.
- de Callafon, R., & Zeng, J. (2006). Recursive filter estimation for feedforward noise cancellation with acoustic coupling. *Journal of Sound and Vibration*, 291(3–5), 1061–1079.
- Denenberg, J. (1992). Anti-noise. *IEEE Potentials*, 11, 36–40.
- Esmailzadeh, E., Alasty, A., & Ohadi, A. (2002). Hybrid active noise control of a one-dimensional acoustic duct. *ASME Journal of Vibration and Acoustics*, 124, 10–18.
- Fuller, C., & Von Flotow, A. (1995). Active control of sound and vibration. *IEEE Control Systems Magazine*, 15(6), 9–19.
- Gee, K., & Sommerfeldt, S. (2003). A compact active control implementation for axial cooling fan noise. *Noise Control Engineering Journal*, 51, 325–334.
- Gentry, C., Guigou, C., & Fuller, C. (1997). Smart foam for applications in passive/active noise radiation control. *Journal of the Acoustical Society of America*, 101, 1771–1778.
- Haykin, S. (2002). *Adaptive filter theory*. Upper Saddle River, New Jersey: Prentice-Hall.
- Heuberger, P., Van Den Hof, P., & Bosgra, O. (1995). A generalized orthonormal basis for linear dynamical systems. *IEEE Transactions on Automatic Control*, 40(3), 451–465.

- Hu, J., & Lin, J. (2000). Feedforward active noise controller design in ducts without independent noise source measurements. *IEEE Transactions on Control System Technology*, 8(3), 443–455.
- Hu, J., Yu, S., & Hsieh, C. (1998). Application of model-matching techniques to feedforward active noise controller design. *IEEE Transactions on Control Systems Technology*, 6(1), 33–42.
- Ljung, L. (1999). *System identification: Theory for the user*. Upper Saddle River, New Jersey: Prentice-Hall.
- O'Brien, M., Pratt, P., & Downing, C. (2002). Active noise control—history, present and future. In *Proceedings of the Irish signals and systems conference* (pp. 59–64), Cork, Ireland.
- Priestley, M. (1981). *Spectral analysis and time series*. London, England: Academic Press.
- Sano, H., & Terai, K. (2003). What is active noise control?. *Journal of the Society of Instrument & Control Engineers* 46, 168–175.
- Wang, C., Tse, C., & Wen, C. (1997). A study of active noise cancellation in ducts. *Mechanical Systems and Signal Processing*, 11(6), 779–790.
- Yuan, J. (2004). A hybrid active noise controller for finite ducts. *Applied Acoustics*, 65(1), 45–57.
- Zeng, J., & de Callafon, R. (2003). Feedforward noise cancellation in an airduct using generalized FIR filter estimation. In *Proceedings of the 42nd IEEE conference on decision and control* (pp. 6392–6397), Maui, HI, USA.